

Arctic Oscillation and ice severity in the Bohai Sea, East Asia

Dao-Yi Gong,^a Seong-Joong Kim^{b,*} and Chang-Hoi Ho^c

^a Key Laboratory of Environmental Change and Natural Disaster, College of Resources Science and Technology, Beijing Normal University, Beijing, 100875, China

^b Korea Polar Research Institute, Incheon, 406-130, Korea

^c School of Earth and Environmental Sciences, Seoul National University, Seoul, 151-742, Korea

Abstract:

The Bohai Sea is the southernmost sea in the Northern Hemisphere where seasonal freezing takes place in winter. Climate and ice conditions there are very sensitive to large-scale climatic variations. In the present study, the authors investigated the relationships of ice severity in the Bohai Sea to the planetary Arctic Oscillation (AO) during the period 1954/55–2001/02. It has been found that during low-AO winters the regional mean temperature around the Bohai Sea is evidently lower, and the number of freezing days, freezing degree days and the length of freezing duration all change significantly. Daily temperature distribution shows a significant difference in both mean and variance between high-AO and low-AO phases, and the changes in the temperature means dominate over that of the variance in the context of sea ice severity. The temperature-AO relation is well supported by the corresponding features of the large-scale atmospheric circulation system. AO-related changes in the Siberian High and East Asian Trough cause remarkable changes to the thermal conditions at the surface and to the dynamical conditions in the middle troposphere, consequently affecting the air temperature over the Bohai Sea and ice severity. The AO-sea ice severity relation has been generally stationary over time during the last one hundred years. Analysis of cross-power coherency between the AO and ice indices for the last century shows that the highest and significant covariance stands at periods of about 2.1, 3, and 7.5–14 years. The Bohai Sea ice severity has declined rapidly since the 1970s, which is unprecedented since 1880, and this feature is in agreement with the positively upward trend in the AO and the associated changes in the Siberian sea level pressure, East Asian Trough, and the regional temperature. Copyright © 2007 Royal Meteorological Society

KEY WORDS arctic oscillation; sea ice; Bohai Sea; climate change; East Asia

Received 2 June 2006; Revised 5 November 2006; Accepted 6 November 2006

INTRODUCTION

The cryosphere is of great significance in global change, both for its large response to the changing climate and as an important mechanism of climate forcing through its feedback (Houghton *et al.*, 2001; Polyakov *et al.*, 2002; Serreze and Francis, 2006). The sea ice in the Northern Hemisphere has experienced an evident decline in its extent and thickness as the climate has warmed over the past few decades (Parkinson *et al.*, 1999; Lindsay and Zhang, 2005; Stroeve, 2005). The Arctic Ocean has been highlighted by many authors for the rapid decrease in the extent of its sea ice in association with recent climate change (Johannessen *et al.*, 2004; Meier *et al.*, 2005; Stroeve, 2005; Overland, 2005). An evident decrease in ice extent is also found in sub-polar regions such as the Baltic Sea, the seas of Okhotsk, the Greenland Sea, Hudson Bay, and the Canadian Archipelago, though an increasing trend has been observed in other areas such as Baffin Bay, the Labrador Sea, the Gulf of St. Lawrence, and the Bering Sea (Parkinson *et al.*, 1999).

These changes in sea ice have been linked to variations of the large-scale atmospheric circulation system e.g. (Deser *et al.*, 2000; Dickson *et al.*, 2000; Rothrock and Zhang, 2005; Brauch and Gerdes, 2005; Wu *et al.*, 2006). It has been found that some remotely located circulation systems play significant roles in high latitude climates through teleconnections (Hurrell, 1996; Thompson and Wallace, 1998), consequently affecting the sea ice conditions in the Arctic and sub-polar oceans e.g. (Koslowski and Glaser, 1999; Jevrejeva and Moore, 2001; Jevrejeva *et al.*, 2003). As a leading mode of Northern Hemispheric atmosphere variability from troposphere to lower stratosphere, the Arctic Oscillation (AO) exerts a notable influence on Northern Hemispheric climates over mid to high latitudes (Thompson and Wallace, 1998, 2000). Observation shows that the AO and North Atlantic Oscillation (NAO) have exhibited a tendency toward positive anomalies during the last two decades (Hurrell, 1995; Thompson *et al.*, 2000). In association with this change, air temperatures in much of the mid to high latitudes have risen and in the Arctic Ocean the sea level pressure (SLP) decreased by 5 mb between the periods 1986–1994 and 1979–1985

*Correspondence to: Seong-Joong Kim, Korea Polar Research Institute, Incheon, 406-130, Korea. E-mail: seongkim@kopri.re.kr

(Walsh *et al.*, 1996). Pressure and wind anomalies related to the AO significantly affect the sea ice motion in the Arctic Ocean and neighboring oceans (Rigor *et al.*, 2002). For example, in the northeastern Atlantic sector, a stronger westerly derived by the enhanced AO or NAO leads to weak ice production, though ice flux through the Fram Strait is enhanced because the SLP gradient between Iceland and Greenland increases, associated with a deeper Iceland Low in winter (Kwok and Rothrock, 1999).

So far, most attention has been paid to high latitude seas. However, in the middle latitudes, temperature and sea ice may respond more sensitively in the context of global warming and the associated changes in atmospheric circulation. In the present study, we address sea ice severity in the Bohai Sea in East Asia (Figure 1), which is the southernmost sea in the northern hemisphere where sea water freezes in boreal winter. A better understanding of sea ice variability in this region is of scientific interest, as it is a sensitive indicator of climate change. Moreover, sea ice in this region is of great economic significance because one of China's economic centers is located around the Bohai Sea, a place where the gross domestic product (in the total as well as per capita) is relatively high. Economic development in this area is highly dependent on the sea conditions and is vulnerable to natural disasters such as bitter winters (Shi, 2003). Heavy sea ice occurs frequently and in extreme cases almost the entire sea is covered by sea ice. Under normal conditions the ice depth ranges from about 40–60 cm in the coastal water to about 10 cm at the extent of the ice edge (Zhang, 1986; Yang, 2000). In winters with heavy ice the ice can be as deep as 1 m or more. Thus, the condition of the sea ice has a great influence on fishing, the oil industry, shipping, and so on, potentially causing tremendous economic losses (Zhang, 1986).

Climate factors, such as the El Niño/Southern Oscillation, western Pacific subtropical high, and so on, are

reported to explain the Bohai Sea ice variability (e.g., Gong and Wang, 2001; Bai *et al.*, 2001; Liu *et al.*, 2004; Li *et al.*, 2005). It seems that the importance of high latitude circulation systems have been somewhat ignored or underestimated, particularly in winter time, when influence from the tropics becomes less important than in summer. Additionally, as a dominant circulation system, the AO plays a very important role in the Northern Hemispheric extra-tropic climate (Thompson and Wallace, 1998; Thompson *et al.*, 2000) and East Asia (Gong *et al.*, 2001; Wu and Wang, 2002; Jeong and Ho, 2005). The AO's impact on ice conditions in the Bohai Sea, however, has not been addressed in previous studies. In the present work we aim to investigate the relation between them.

In Section 2 we describe the data employed, including the sea ice severity index, temperature, and atmospheric circulation. The coherence between sea ice and air temperature is presented in Section 3. The variability of temperature and atmospheric circulation in association with the AO is analyzed in Section 4. Long-term changes in temperature and the circulation in the context of ice severity are examined in Section 5. Finally, the conclusions of the study are summarized in Section 6.

DATA AND METHOD

Sea ice severity index

The Bohai Sea is located off northeast China, from about 37–41°N to 117–123°E, and is surrounded by land to the west, north, south, and northeast (Figure 1). It opens to the Yellow Sea only in the southeast by way of the Bohai Strait. On average, the water depth is 18 m. In such a half-enclosed and very shallow sea, the local weather plays an essential role in sea ice conditions. Observations indicate that, in this particular region, the dynamical factors such as wind stress and surface ocean currents are not so important in the distribution of sea ice (Zhang,

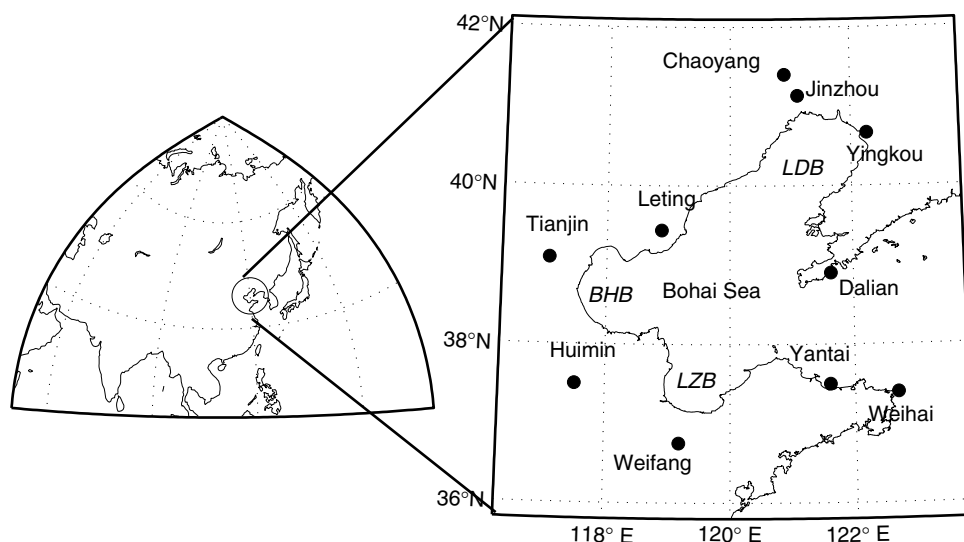


Figure 1. Study area and meteorological stations. BHB: Bohai Bay, LDB: Liaodong Bay, LZB: Laizhou Bay.

1986). In the present study, thus, we do not address the influence of wind related ice-dynamics. We focus only on the sea ice severity due to temperature variability.

The operational observation and prediction of sea ice in northern China began in the middle 1950s. To monitor the sea ice in northern coastal waters, the State Oceanic Administration (SOA, 1974) defined five categories of sea ice severity on the basis of the ice depth and the maximum coverage of fixed and floating ice. According to the maximum ice extents along the axes of Liaodong, Bohai, and Laizhou Bays (see Figure 1), their respective sea ice severity were determined, then the three severity indices were averaged to make a single index for the entire sea. The five categories vary from 1.0 to 5.0. Category 1 represents the lightest ice severity, 5 the most severe, 3 the normal, and categories 2 and 4 denote the moderately light and moderately heavy severities, respectively. During extreme conditions (category 5), most of the sea is covered by sea ice. In the present study, the sea ice severity index is taken from (Bai *et al.*, 2001) for the period 1953/54–2000/01. This data set has been updated further, for the period 2001/02–2004/05, in this study, on the basis of the State Oceanic Administration's annual bulletin of ocean disasters. It is available at <http://www.soa.gov.cn>, and the relevant figures or satellite imageries of ice extent in association with the ice severity category can also be found there. So, the sea ice time series covers winters for the period 1953/54–2004/05 (Figure 2).

Meteorological data

Daily temperature for eight stations around the sea are obtained from the China Meteorological Administration (Figure 1 and Table I). All data cover the period of 1954–2002, except the data for Leting, which are available for 1957–2002. During the sampling period, there are few missing days in six stations (Jinzhou, Yingkou, Dalian, Huimin, Weihai, and Weifang). In these stations the missed data occurred on the same days, namely 29 November 1955, and 29–30 December 1967. These missing data have been filled on the basis of observations at neighboring stations (e.g. Figure 3).

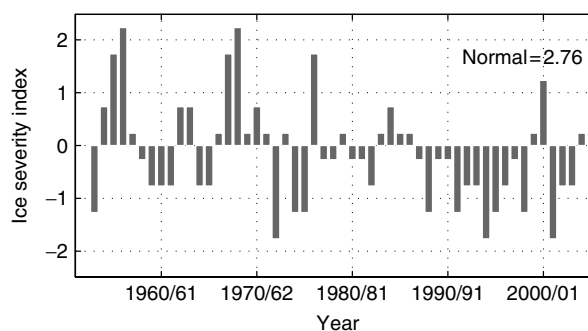


Figure 2. Time series of the Bohai Sea ice severity index for the winters 1953/54–2004/05. Shown as departures from the normal of 2.76 for the reference period 1961–90.

In addition to the aforementioned eight stations, we also used the seasonal mean temperature (December–February) for four stations (Tianjin, Dalian, Yantai, and Chaoyang) whose data periods extend back to 1880 (Table I).

Northern Hemisphere tropospheric data used here are taken from the European Centre for Medium-Range Weather Forecast (ECMWF) 40-year reanalysis (ERA40) (Uppala, 2005), and includes heights, wind vector, and temperature from 1000 hPa to 100 hPa levels. ERA40 covers the period September 1957–August 2002 and is archived on a $2.5^\circ \times 2.5^\circ$ longitude–latitude grid. The data are available six-hourly. In the present study, we used only the data received at 0600UTC. Monthly circulation data were obtained by averaging daily data.

The AO index is the corresponding time coefficient of the first empirical orthogonal function of the monthly SLP (northward of 20°N), and available since 1899 (Thompson and Wallace, 1998).

We also used SLP data from the Met Office Hadley Centre, HadSLP2, which is a newly released data set consisting of monthly fields of global land and marine pressure on a 5-degree latitude–longitude grid covering the years 1850 to 2004 for details see (Allan and Ansell, 2006).

Regression analysis

To reveal the relationship between the sea ice severity index and the temperature and atmospheric circulation

Table I. Meteorological stations of temperature used in the present study.

Name	WMO code	Location	Altitude	Daily temperature (1 November–31 March)	Winter mean temperature (December–February)
Tianjin	54 527	39.08°N, 117.07°E	2.5 m	1954–2002	1880–2004
Leting	54 539	39.43°N, 118.88°E	10.5 m	1957–2002	no
Jinzhou	54 337	41.13°N, 121.12°E	65.9 m	1954–2002	no
Yingkou	54 471	40.67°N, 122.27°E	3.3 m	1954–2002	no
Dalian	54 662	38.90°N, 121.63°E	91.5 m	1954–2002	1880–2004
Huimin	54 725	37.50°N, 117.52°E	11.7 m	1954–2002	no
Weihai	54 776	37.40°N, 122.68°E	47.7 m	1954–2002	no
Weifang	54 843	36.75°N, 119.18°E	22.2 m	1954–2002	no
Yantai	54 751	37.53°N, 121.40°E	47.0 m	no	1880–2004
Chaoyang	54 324	41.55°N, 120.45°E	169.9 m	no	1880–2004

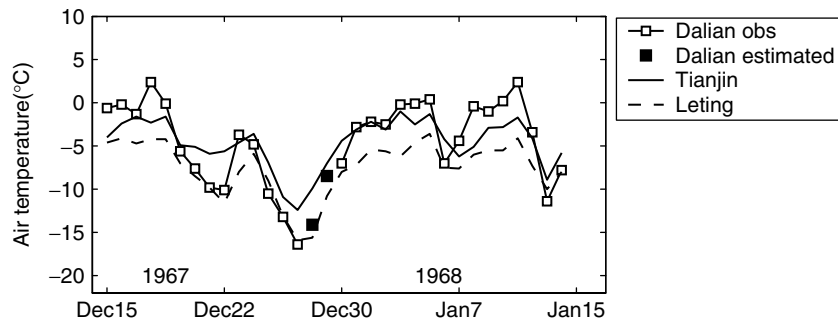


Figure 3. Time series of the temperature of Dalian from 15 December 1967 through 15 January 1968. Compared with the simultaneous temperatures of Tianjin and Leting, these two stations are used to estimate the missing data in Dalian and the other five stations.

in the Northern Hemisphere, a regression analysis is performed. In this analysis, the sea ice severity index anomaly is specified as one standard deviation, so that the regression coefficients always correspond to the same unit change of the independent variable. When analyzing temperature and circulation associated with the change in the AO, the same method is applied. The confidence level of their regression relations is judged by a two-tailed t -statistic. A strong trend and low frequency would evidently reduce the effective degree of freedom, which is a critical parameter in determining confidence levels. To avoid any overestimation, we applied the (Bretherton *et al.*, 1999) method to calculate the effective degree of freedom by computing the auto-correlation of the time series. By this method, the number of degrees of freedom is shorter by about eight than the sample length of the ice severity index.

In addition, the field significance of the regression maps including the 925 hPa temperature, 850 hPa wind, SLP, and 500 hPa heights, as shown in the later sections, are tested using Monte Carlo method. The critical numbers of grids for a 0.05 level vary in the range 11–19% for these maps.

SEA ICE SEVERITY AND AIR TEMPERATURE

Variation in sea ice severity

Figure 2 shows the time series of the ice severity index for the 52-year period. Strong year-to-year fluctuations as well as long-term trends are clearly evident. Over the data period, the variance of the original index is 0.98. Interannual variance with a timescale less than 10 years contributes about two-thirds of this, as estimated from the results of a high-pass Butterworth filter. During

the total of 52 winters, the six most serious sea ice extremes with a severity above category 4.0 occurred in 1955/56, 1956/57, 1967/68, 1968/69, 1976/77, and 2000/01. Among them, the winter of 1968/1969 is the most remarkable with regard to its impact. In that winter, the sea ice covered almost the entire Bohai Sea, resulting in great economic loss. More than 400 fishing vessels with about 1500 workers onboard were stranded in the sea by the heavy ice, and one oil drilling platform was completely destroyed and two others were heavily damaged (Zhang, 1986).

The other one-third of the total variance in sea ice severity is accounted for by low-frequency variations longer than 10 years. As seen in the figure, greater ice severity takes place frequently in some periods: severity peaks in the mid 1950s, late 1960s, and 1976. Also, it is noted that the secular trend accounts for a large portion of the low-frequency variations. The linear trend estimated using a least squared error technique is -0.29 per 10 years (Table II). This significant change rate, in the absolute value, is about 30% of the standard deviation of the ice severity index. Thus, the ice severity is becoming significantly lighter, and ice coverage is getting smaller.

To examine the details of the temporal features, we checked the dominant frequencies using power spectral analysis. The variations with time scales of 2.7, 3.3, 6.7, and 13.3 years are outstanding in power spectral density, although none of them are statistically significant at the 0.05 level. Some previous studies found similar time scales in the Bohai Sea ice conditions (Bai *et al.*, 2001; Li *et al.*, 2005). It is interesting to note that AO and NAO consists of similar leading signals with time cycles of about 2.2–2.4, 7.8, and 12.8 years (Hurrell

Table II. Trends in climate time series during the period 1954/55–2001/02. Unit: Per Decade.

Sea ice	AO (Dec.–Feb.)	Mean temperature (Dec.–Feb.)	Number of freezing days (Dec.–Feb.)	Freezing degree days (Dec.–Feb.)	Freezing duration (Nov.–Mar.)
-0.29^a	$+0.34^a$ ($+0.27^{a,c}$)	$+0.42\text{ }^\circ\text{C}^a$	-3.6 days^a	$+32.5\text{ }^\circ\text{C days}^a$	-3.8 days^b

^a Significant at $\alpha = 0.01$ level.

^b At 0.05 level.

^c For 1954/55–2004/05.

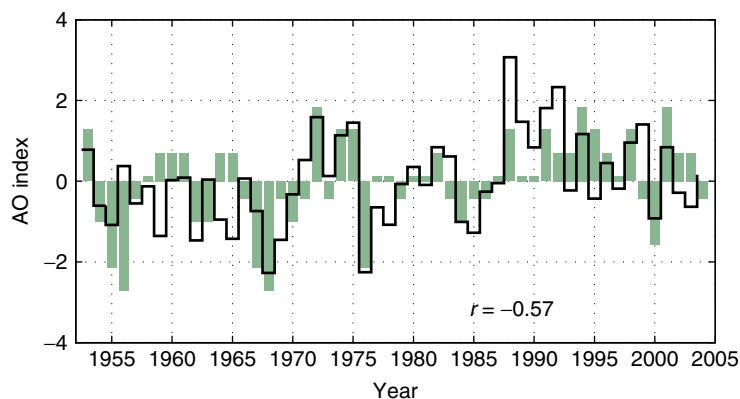


Figure 4. Time series of the December–February AO index (solid line), along with Bohai Sea ice severity appearing as bars, which is normalized and multiplied by minus one. This figure is available in colour online at www.interscience.wiley.com/ijoc

and van Loon, 1997; Jevrejeva and Moore, 2001). With regard to AO variability, Baltic Sea ice conditions during the past 150 years are mainly associated with signals in the 2.2–3.5, 5.7–7.8, and 12.8 year bands (Jevrejeva *et al.*, 2003), comparable with the Bohai Sea ice severity results.

The relation between AO and the Bohai Sea ice severity is clearly identified by comparing their time series (Figure 4). Since two variables have an out-of-phase correlation, to facilitate comparison of the figures, the ice index has been normalized and multiplied by -1 . The two series then show very good agreement, that is, some severe ice winters are accompanied with AO minima, such as the winters of 1968/69, 1976/77, and 2000/01. Two of the curves are significantly correlated with a Pearson correlation coefficient of $r = -0.57$ ($r^2 = 32\%$). Even after removal of the notable long-term trends, which have an excessive impact on the degree of freedom, the interannual components of these two variables are correlated with a strong correlation of $r = -0.51$ ($r^2 = 26\%$), still significant at the $\alpha = 0.01$ level, suggesting that their association in variability is statistically robust.

Air temperature

A large drop in air temperature, related to the strong East Asian winter monsoon, can easily cool the sea surface below freezing point and consequently result in the formation of sea ice in the coastal waters. One outstanding feature in East Asian climate change is the significant warming in winter. Particularly, the north portion of East Asia (includes the target region) has experienced a larger warming trend than the south (Wang and Gong, 2000; Wang *et al.*, 2001). Here we examine the mean temperature variability in winter (December through February) when sea ice reaches its maximum extent. Averaging from daily air temperature readings of eight stations that are located around the Bohai Sea (Table I), we obtained the mean temperature time series, $\bar{T} = \frac{1}{n} \sum_{i=1}^n T_i$, where T_i is the daily mean temperature, and n is the number

of days from December 1st through to 28/29 February. The calculation is done for each station each winter. Figure 5a shows the mean temperature anomalies in December–February. The two time series are correlated at $r = -0.77$, $r^2 = 59\%$ (Table III), being a fairly well inverse relationship. The peaks of the sea ice severity (such as in 1956/57, 1968/69, and 2000/01) correspond very well to temperature minima. As the winter mean temperature has increased at the rate of $+0.42^\circ\text{C}$ per 10 years during the last couple of decades, the sea ice severity rapidly declined correspondingly. Mean temperature alone accounts for about 60% of the ice severity variance. Extreme temperature events occurred frequently in the most recent two decades. The winters of 1998/99 and 2001/02 rank as the warmest cases since the 1950s, accompanied with ice severity minima. China experienced the warmest year in 1998, and much of the warming occurred in the northern winter season (Gong and Wang, 1999a; Wang *et al.*, 2001) meanwhile notably thin ice conditions were observed in the Bohai Sea (Meng and Li, 1999). Dalian station documented the highest temperature anomaly in the winter of 1998/99 since records began in 1905, and ice melted about 20 days earlier than normal (Meng and Li, 1999). The maximum ice extent in the Liaodong Bay was 59 nautical miles, while in the Bohai and Laizhou Bays the maximum ice width was 10 and 3 nautical miles, respectively. The ice maximum was observed on 15 January 1999. Averaging from the

Table III. Correlation among climate indices for the period 1954/55–2001/02^a.

	\bar{T}	Number of freezing days	Freezing degree days	Freezing duration ^b
Ice severity index	-0.77	+0.77	-0.84	+0.47
AO index	+0.46	-0.50	+0.54	-0.25
Siberian High	-0.73	+0.73	-0.78	+0.56
Trough index	+0.69	-0.67	+0.72	-0.55

^a All values are significant at $\alpha = 0.01$ level, except for the correlation between AO and the freezing duration of which the level is $\alpha = 0.1$.

^b November–March.

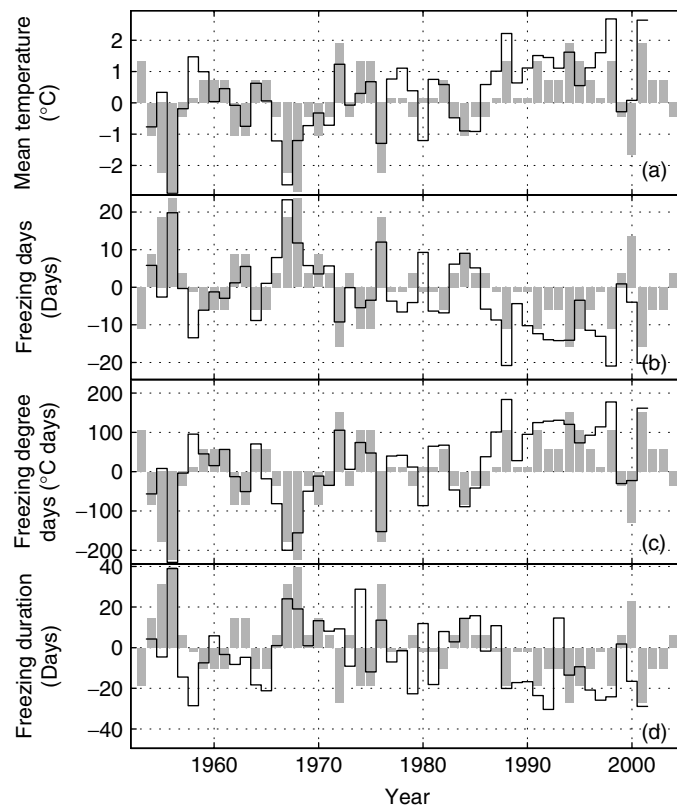


Figure 5. Time series of the temperature indices shown in solid lines as departures from the reference period of 1961–1990. (a) mean temperature, (b) number of freezing days, (c) freezing degree days, (d) freezing duration. The ice severity index are shown as bars for comparison. To facilitate comparison, the ice indices in (a) and (c) have been multiplied by minus one and arbitrarily rescaled.

Table IV. Bohai Sea ice conditions and the temperature in winters 1998/99 and 2000/01.

	Liaodong Bay	Bohai Bay	Laizhou Bay	Temperature anomaly
Winter of 1998/1999:	–	–	–	–
Maximum width (nautical mile)	58	10	3	–
Date of maximum extent	15 January 1999	–	–	+2.6 °C (+1.9 σ) ^a
Ice severity	1.5	–	–	–
Winter of 2000/2001:	–	–	–	–
Maximum width (nautical mile)	115	30	~5	–
Date of maximum extent	7–13 February 2001	–	–	–0.1 °C (–0.05 σ) ^b
Ice severity	4	–	–	–

^a January.

^b February.

σ is the standard deviation for 1961–1990 reference period.

eight stations, the monthly mean temperature in January 1999 is -2.2 °C (anomaly is $+2.6$ °C), about 1.9σ above the 1961–1990 reference normal (Zhang and Li, 1999; Meng and Li, 1999). It should be noted that in some winters the surface air temperature was only slightly below the normal but a severe ice condition took place, such as in winter of 2000/01 when the most severe ice condition occurred since the 1980s (Table IV). This may be due to several strong cold surges in association with extreme weather conditions. This could also be due to the change in sea ice dynamics, i.e. the distribution of ice could be governed by a strong wind. The floating sea ice moves at an average velocity of 0.3–0.5 m/s, and its

dominant moving path/direction is northeast–southwest, nearly parallel to the western coast (Zhang, 1986; Bai *et al.*, 1999). Therefore, the influence of wind on ice extent is not as important as temperature.

Sea ice often exists on many of the winter days. On average, sea ice appears first in the Liaodong Bay in late November, in the Bohai Bay in middle December, and in the Laizhou Bay in late December, whereas it disappears in middle March in the Liaodong Bay and in late February in the Bohai and Laizhou Bays. Thus, the duration of freezing (which may be separated by some relatively warm days) is about 100 days on the northern coast and 60 days in the southwest, respectively (Bai *et al.*, 1999).

Using daily air temperature here, we checked the duration of freezing, which is defined as the length between the first freezing spell and the last freezing spell during the period 1 November–31 March. The start of a freezing spell is counted when five consecutive days with a daily mean temperature below -4°C is observed. One freezing duration may consist of some short freezing spells, but between these freezing spells the temperature can be close to zero or even above zero in Celsius. It should be pointed out that in the present study the length of freezing duration is defined on the basis of air temperature, not on the presence of sea ice. This air temperature derived length of freezing duration is somewhat shorter than that for the sea ice observations, this is because the freezing of seawater depends not only on the temperature, but also on salinity. The salinity of coastal waters is low, thus freezing can take place at a higher temperature, subject to location and weather (Zhang, 1986). For example, in northern Liaodong Bay the freezing temperature of water is about -1.4°C (Li, 1999). (Gu *et al.*, 2003) also employed a threshold of -2°C to estimate the Bohai Sea ice amount. To highlight the ice severity, however, in this study we used an air temperature of -4°C , which is a somewhat stricter criterion. Generally, the ice severity varies in phase with the length of freezing duration with a correlation of $+0.47$, suggesting that severe ice conditions tend to occur in longer freezing duration winters. Since the 1950s, the freezing duration has been decreasing at a significant rate of -3.8 days in 10 years, thus during the last 48 years, the freezing duration has shortened by 18.2 days.

In addition to the mean temperature and freezing duration, we further checked another two temperature indicators, namely, the freezing degree days (FDDs), and number of freezing days (NFD). Here, FDD and NFD are respectively defined as follows:

$$FDD = \sum_{i=1}^n T_i, \quad (T_i \leq -4^{\circ}\text{C}) \quad (1)$$

$$NFD = \sum_{i=1}^n \delta_i, \quad (\delta_i = 1 \text{ if } T_i \leq -4^{\circ}\text{C}) \\ \delta_i = 0 \text{ otherwise) } \quad (2)$$

where T_i is the daily temperature and n is the number of days from 1 December through to the next 28 February (or 29 February in leap years). As seen from the two equations above, NFD counts the number of days in which the daily mean temperature is below freezing point. FDD represents the accumulated freezing temperatures from all freezing days in each winter, and to some extent it reflects the accumulated air temperature coldness. Both NFD and FDD show a strong correlation to the sea ice severity index, with correlation coefficients of $+0.77$ ($r^2 = 59\%$) and -0.84 ($r^2 = 71\%$), respectively (Figures 5(c) and 5(d)). Generally, the maxima and minima in these four temperature indices are consistent

with each other as well as with the ice conditions. Compared to the mean temperature, the FDD represents ice severity with a more physical meaning. As the accumulated FDDs depict the extent to which these days get cold, it is an important indicator of the sea ice amount (Gu *et al.*, 2002). The highly in-phase variations between sea ice index and FDD are most outstanding, as can be seen in Figure 5. The positive trend of FDD ($+32.5\%$ per 10 years) suggests a rapid decrease in the coldness, which plays an essential role in the reduction of sea ice severity.

In deep and open oceans, the sea water responds to atmosphere with a certain time lag (usually varying from 1 to 2 months). However, the condition in the shallow Bohai Sea is very different. We computed the possible time lags between sea ice and temperatures. Analysis shows that, among all possible time lags, the simultaneous correlation is the highest. This may be because of the fact that the Bohai Sea is very shallow and well mixed all the time and the sea ice here is mainly controlled by the regional weather. Therefore, it seems that the long-term warming trend and the associated decrease in NFD, FDD, and length of freezing duration in north China is directly and chiefly responsible for the decrease in the sea ice severity in the Bohai Sea.

RELATIONS TO AO

Local temperature changes

Changes in both temperature mean and temperature variance can impact the length of freezing duration, FDD, and NFD, and as a consequence, influence sea ice conditions. Many previous studies have indicated that the temperature in East Asia is highly linked to the AO phases, the mean temperature being warmer than normal and the high frequency variance of temperature becoming smaller during positive-AO winters (Gong and Ho, 2004; Gong *et al.*, 2004). To understand better how local temperatures respond to AO, we analyzed the temperature statistics of the daily data. Because variance and means differ from station to station, only two stations (Jinzhou and Dalian) are taken as examples here. First of all, the high-AO and low-AO phase years during the period 1954/55–2001/02 are identified with respect to its anomaly:

- (1) Seven high-AO winters with AO index larger than $+1.2\sigma$: 1972, 1975, 1988, 1989, 1991, 1992, and 1999;
- (2) Six low-AO winters with AO index smaller than -1.2σ : 1959, 1962, 1965, 1968, 1969, and 1976.

The remaining winters are AO-neutral years. Table V summarizes the mean temperature, variance, and temperature-related ice parameters at two stations, Jinzhou and Dalian. In these two stations the mean temperature for high-AO winters is significantly greater than the mean temperature for low-AO winters, 1.9°C

Table V. Statistics for two stations' daily mean temperature in association with AO index.

	Mean (°C)	Variance (°C ²)	Number of freezing days (Days)	Freezing degree days (°C days)	Freezing duration (Days)
Jinzhou:					
High-AO	-5.3	17.8	56.7	-444.5	60.4
Low-AO	-7.2	24.8	66.5	-625.9	81.8
High-low	1.9 ^a		-9.8 ^a	181.4 ^a	-21.4 ^b
Low/High		1.4 ^a			
Dalian:					
High-AO	-1.7	18.2	25.7	-177.4	20.2
Low-AO	-3.5	30.4	40.5	-345.2	37.3
High-low	1.8 ^a		-14.8 ^a	167.8 ^a	-17.2
Low/High		1.7 ^a			

^a Significant at 0.05 level.

^b At 0.1.

in Jinzhou and 1.8°C in Dalian, respectively. The corresponding decrease in NFD and freezing duration, and mitigation of FDD are evident in the two stations. It is interesting to note that the temperature variance is notably different between high-AO and low-AO winters (Figure 6). At first glance, we find that the temperature distribution in low-AO winters tends to have a broader span, while the peak of probability density function (PDF) is smaller than the peak for high-AO PDF, suggesting that the daily temperature in low-AO winters is more variable than in high-AO years. The variance difference between high-AO and low-AO winters, estimated using F-statistics, shows that both Jinzhou and Dalian are significant at the 0.05 level. Our analysis indicates that AO-associated changes in both temperature mean and temperature variance are important.

The observed changes in NFD and FDD and ice conditions may be due to the combined effects of temperature mean and variance. To obtain an idea about the extent to which each of them impacts the number of freezing days and FDDs, we employed a theoretical

computation. The theoretical PDF is determined by the observed mean (μ) and standard deviation (σ) on the assumption that the temperature (T) obeys the normal distribution:

$$PDF = y(T|\mu,\sigma) = \frac{1}{\sigma\sqrt{2\pi}} e^{-\frac{(T-\mu)^2}{2\sigma^2}} \quad (3)$$

Taking into account the length of winter ($L = 90$ days), the theoretical number of freezing days and FDDs can simply be computed. Subject to the observed values of the mean and standard deviation in high-AO and low-AO winters, the NFD and FDD changes due to the changes of μ and/or σ can be separately estimated as given below:

$$\Delta NFD = 90 \left(\int_{-\infty}^{-4^\circ\text{C}} y_+ dT \right) - \int_{-\infty}^{-4^\circ\text{C}} y_- dT \quad (4)$$

$$\Delta FDD = 90 \left(\int_{-\infty}^{-4^\circ\text{C}} T y_+ dT - \int_{-\infty}^{-4^\circ\text{C}} T y_- dT \right) \quad (5)$$

where y_+ and y_- denote the PDF in association with high-AO and low-AO winters, respectively. Results are shown in Table VI. For Dalian, the NFD difference between high-AO and low-AO winters is -14.7 days. $\Delta\mu$ and $\Delta\sigma$ contributes -13.0 and -1.7 days, respectively. Similarly, about 70% of the FDD changes are due to the changes in μ , while the contribution by $\Delta\sigma$ is

Table VI. Theoretical changes in the number of freezing days (ΔNFD), and the freezing degree days (ΔFDD) due to temperature mean (μ) and standard deviation (σ) differences between high-AO and low-AO winters (high minus low).

	$\Delta\mu$ alone	$\Delta\sigma$ alone	$\Delta\mu + \Delta\sigma$
Jinzhou			
ΔNFD (days)	-12.4	3.0	-9.5
ΔFDD (°C Days)	166.8	12.0	179.2
Dalian			
ΔNFD (days)	-13.0	-1.7	-14.7
ΔFDD (°C Days)	114.6	49.8	163.8

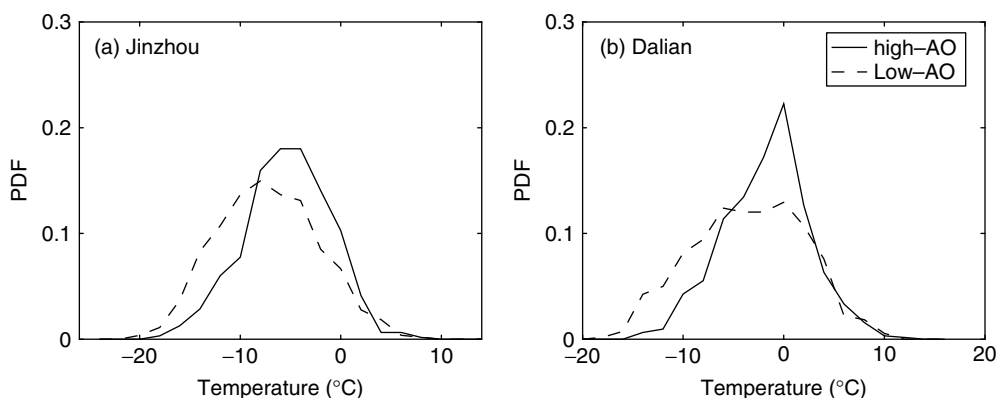


Figure 6. Probability density function (PDF) for daily mean temperature of Jinzhou and Dalian, showing the difference between the high-AO and low-AO winters.

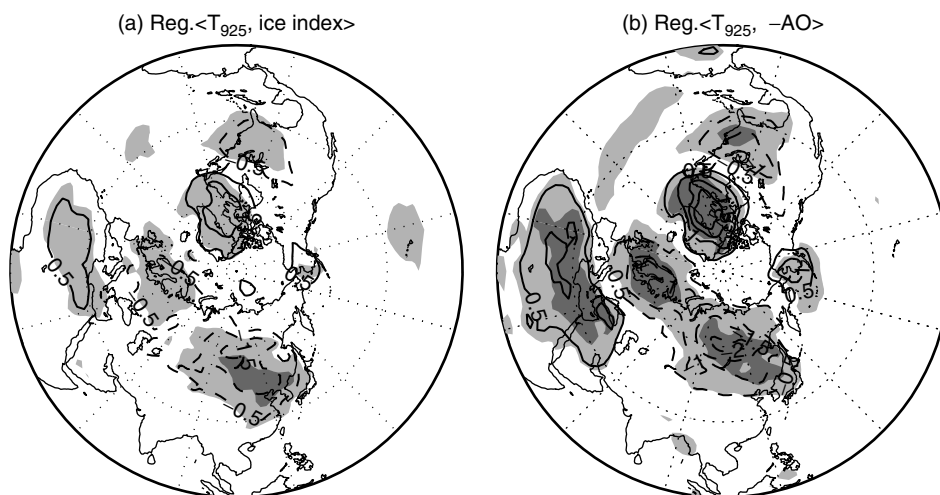


Figure 7. Changes of air temperature at the 925 hPa level in December–February in association with a one-standard-deviation stronger sea ice severity index (a) and AO (b), based on the data period of winters 1957/58–2001/02. Areas significant at 0.05 level are shaded and the high correlation center with $|r| \geq 0.6$ indicated by darker shading. Contour intervals: 0.5°C . Zero lines are omitted for clarity.

much weaker, though the variance itself changes significantly from high-AO winters to the lows. The influence of the variance on FDD is somewhat greater than that on NFD because it impacts much more on the extreme temperatures. The evident influence of $\Delta\sigma$ can also be found in the case of Jinzhou. It is very interesting to note that in Jinzhou a smaller variance in high-AO winters gives rise to about three more freezing days, in contrast to the conditions in Dalian, where the smaller σ causes a drop of -1.7 days in NFD. This is due to the fact that the Jinzhou mean temperatures in both high-AO and low-AO winters are below the critical point of -4°C , and so a smaller temperature variance in high-AO winters results in less warmer temperature days. Since the critical point of -4°C is located on the warmer half (i.e. the right side) in the PDF, the number of cold days increases as a consequence. This indicates that the climate indices may respond to variance changes in different (even opposite) ways, depending on how the critical points or standards are selected. Overall, the above analysis suggests that, compared to the variance, the mean changes in temperature in association with AO phases have a more important influence on air temperature indices and ice conditions.

Large-scale temperature anomalies

In the previous section, we showed that there is a modest association between the AO and sea ice severity, as suggested by their r^2 of 32%. Temperature plays an essential role in the Bohai Sea ice. Thus the AO influence, if any, in a physical sense, should be supported by a large-scale climate anomaly in the context of the Bohai Sea ice. To verify this, we first regressed the December–February air temperatures at the 925 hPa level over the whole Northern Hemisphere on the ice severity index. The results (Figure 7(a)) show that there is a clearly well-defined spatial pattern on a hemispheric scale. In association with heavier ice severity, the air temperature is 0.5 – 1°C lower in the middle-high latitudes of Asia

and anomalies of about -0.5°C appear in northern and eastern Europe. Meanwhile, the temperatures in northern Africa and Greenland rise above 0.5°C . These features resemble the general structure of AO-related temperature anomalies (see relevant figures Hurrell and van Loon, 1997; Thompson and Wallace, 2000). For comparison, we plotted the AO regression maps (Figure 7(b)). Both maps are significant at a 0.05 level, as confirmed by the field significance test. A similarity in the spatial pattern between the sea ice severity and AO is impressive, especially in mid-high-latitudes. In the case of weaker AO winters by one standard deviation, negative temperature anomalies (-0.5 to -1.5°C) appear in mid-latitude Asia, Europe, and the southeastern U.S., while strong positive anomalies take place in northern Atlantic ($\geq +2\text{C}$) and northern Africa ($+0.5$ to $+1.0^{\circ}\text{C}$). This evidence suggests that severe ice conditions in the Bohai Sea tend to occur when AO is in its negative phases, while light ice conditions tend to appear in positive-AO winters. Clearly, the Bohai Sea air temperature anomaly is a local manifestation of hemispheric changes in the context of AO.

Thompson and Wallace (2000) demonstrated that a lot of the AO-related temperature anomalies are associated with horizontal heat advection due to the zonal component of the air-flow. However, in East Asia an opposite advection appears in the south of the Bohai Sea and in the areas north of it (see Figure 11 in the reference cited). Around the Bohai Sea the temperature advection due to zonal winds is not obvious. Thus, it is unlikely that the zonal heat transport can explain the significant temperature change over northern China. Previous studies have reported that AO exerts an obvious influence on East Asia through the winter monsoon (Gong *et al.*, 2001; Wu and Wang, 2002), while in the lower troposphere the winter monsoon is characterized by a dominant meridional circulation, as supported by the presence of a remarkable horizontal wind at 850 hPa (Figure 8). During negative AO winters, an anomalous north wind is

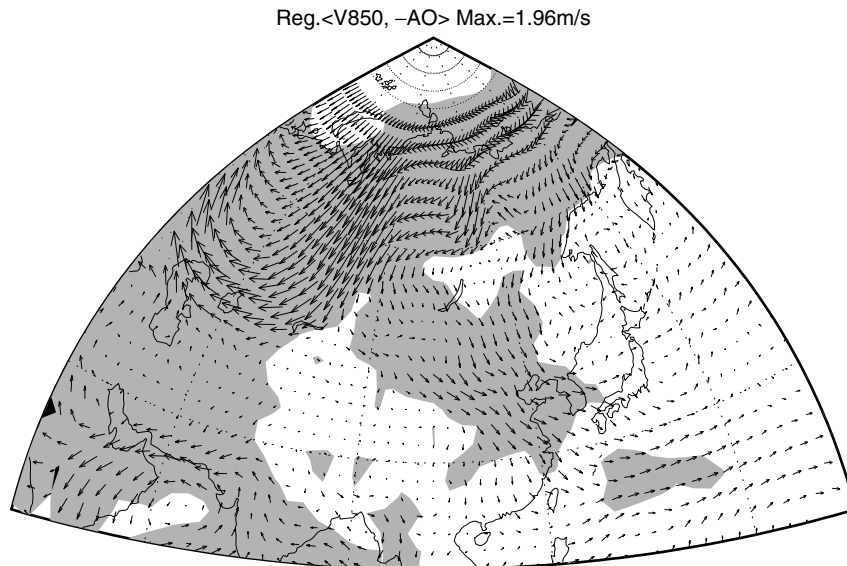


Figure 8. Changes in horizontal wind at the 850 hPa level in December–February in association with a one-standard-deviation weaker AO index, based on the data period of winters 1957/58–2001/02. Shading indicates either zonal(u) or meridional(v) wind that is significant at the 0.05 level.

observed over the whole of East Asia. Two major paths are clear. One path is the original source of the anomalous northerly winds that is located in western Siberia: a northerly wind anomaly is found along about 90°E , which then turns northwesterly, and finally appears as an anomalous northerly wind in East Asia. The other source is located in the east of Siberia: anomalous northerly flow originates from there and reaches East Asia along $120\text{--}130^\circ\text{E}$.

A pressure-height section along 120°E shows that the colder temperature in heavy ice conditions occurs between $30\text{--}60^\circ\text{N}$, with its center at about 45°N , and extends from the surface up to the 400 hPa level. Note that heat transport by the north wind appears to be important below 700 hPa, while between 400–700 hPa the north wind transport is weak (Figure 9). Interestingly, the changes in circulation in association with AO also show very similar features (Figure 10). An anomalous low temperature anomaly at $35\text{--}75^\circ\text{N}$ extends from the surface to 400 hPa and the anomalous north wind is evident below about 700 hPa. On a planetary scale, the AO-related zonal wind dominates from the lower troposphere to the lower stratosphere (Thompson and Wallace, 2000), and the cold temperature anomaly between 700 and 400 hPa is likely due to the zonal/vertical heat transport. However, near the land surface, the meridional transport is dominant. These features are also supported by the changes in the zonal mean wind (u). The upper troposphere westerly wind (particularly the jet stream) is stronger in negative AO phases and heavy ice winters. This is consistent with previous studies (Ambaum *et al.*, 2001; Chen *et al.*, 2003). All the evidence suggests that the large-scale AO plays a very important role in the Northern Hemisphere temperature changes, including in East Asia.

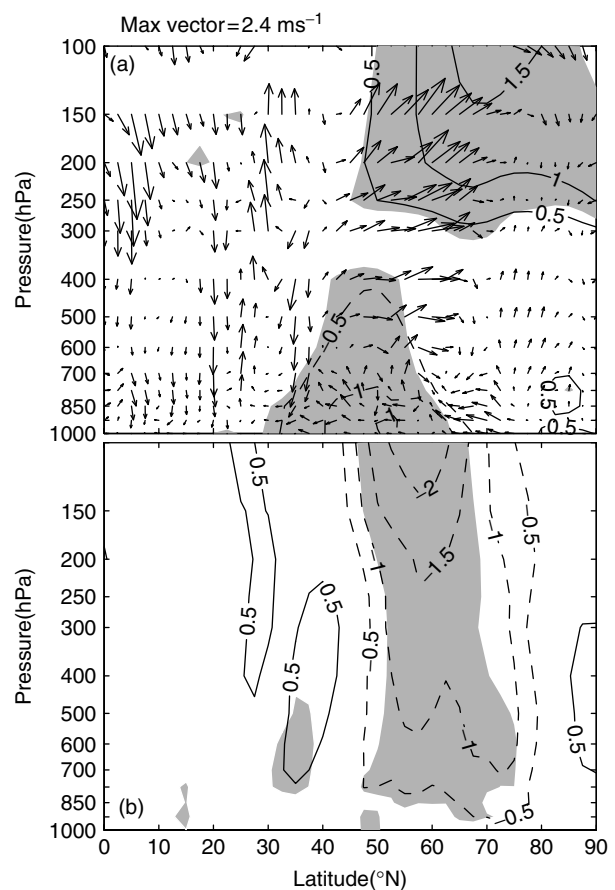


Figure 9. Regression of wind and temperature along the 120°E section in troposphere (from 1000hPa to 100hPa) on the sea ice severity index. In (a), the temperatures are shown in contour lines with interval of 0.5°C , shading area denotes the 0.05 significance level. Meridional (v) and vertical (w) motion are shown as vectors, w has been multiplied by 10. Zonal wind (u) anomalies are shown in (b), with significant (at 0.05 level) areas shaded.

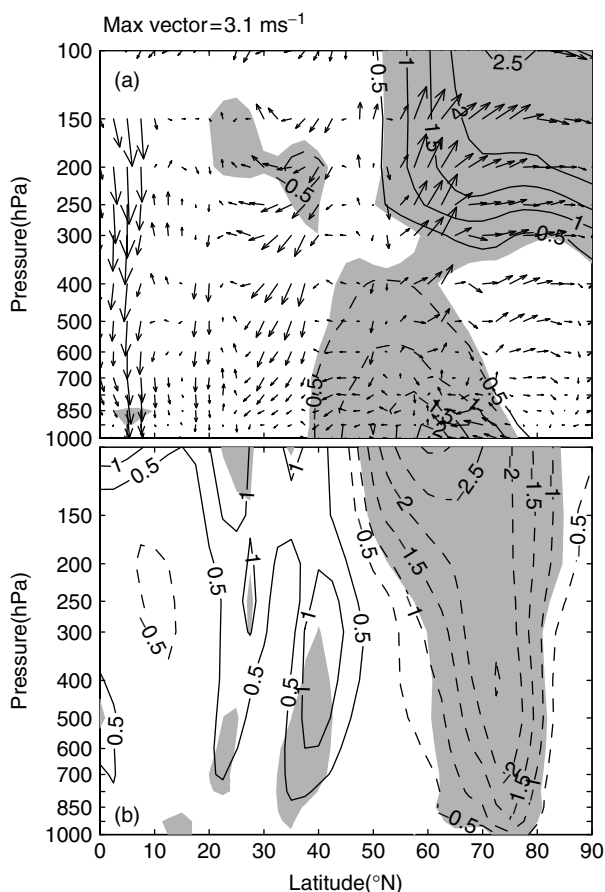


Figure 10. Same as in Figure 9, but for regression upon the AO index. Here, the AO index has been multiplied by -1 to facilitate comparison.

Sea level pressure

The AO is defined by SLP fields and thus reflects the change in regional SLP. During winter, the dominant circulation system near the surface of the Eurasian continent is the Siberian High, which exerts considerable influence on climate in mid-high-latitudes (Gong and Ho, 2002; Panagiotopoulos *et al.*, 2005), and explains about 43% of the temperature variance in East China during the last one hundred years (Gong and Wang, 1999b). Previous studies reported that there is a significant out-of-phase relationship between the AO and the intensity of the Siberian High (Gong *et al.*, 2001; Wu and Wang, 2002; Gong and Ho, 2002). It is worth investigating how the AO-related SLP changes are related to the Bohai Sea ice severity.

The HadSLP2 SLP anomaly related to the sea ice severity index was determined by linear regression and is presented in Figure 11. In heavy ice winters, the SLP tends to increase in the Arctic Ocean and decrease in the mid-latitudes of the North Atlantic. This is reminiscent of the negative AO pattern. Note that the most significant SLP change is found in Siberia, where the SLP is strongly correlated with the sea ice index above $+0.6$, i.e., $r^2 \geq 36\%$. This regression map is significant at the 0.05 level by the field significance test. In order to look for more detail, we simply defined

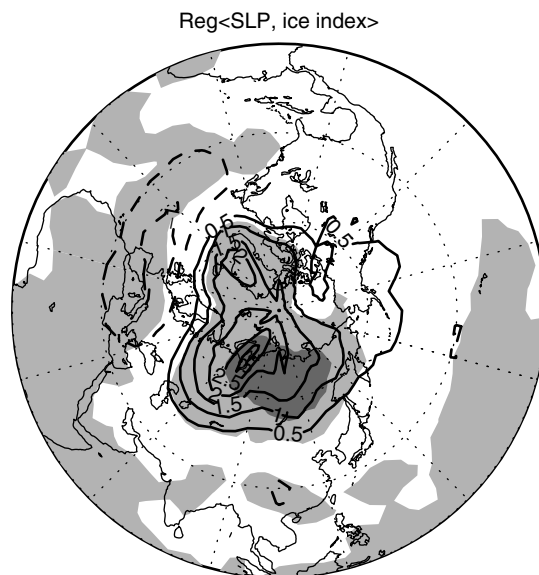


Figure 11. Changes of December–February SLP (HadSLP2) in association with a one-standard-deviation stronger sea ice severity index, based on the data period of winters 1953/54–2003/04. Areas significant at the 0.05 level are shaded. High correlation center with $|r|$ above 0.6 is indicated by darker shading. Contour interval: 0.5 hPa. Zero contours are omitted for clarity.

a Siberian High index as the regional mean SLP in $70\text{--}140^\circ\text{E}$ and $55\text{--}70^\circ\text{N}$ where the most significant correlations are located. The domain mean temperature and FDD are well correlated with the Siberian SLP at -0.73 ($r^2 = 53\%$) and -0.78 ($r^2 = 61\%$), respectively. Comparable correlation coefficients are found in the NFD and the length of freezing duration (Table III). This is consistent with previous studies in which a tight relationship between the Siberian High and East Asian temperatures was obtained, similar to this study (e.g., Gong and Wang, 1999b; Wu and Wang, 2002). Furthermore, the Siberian SLP variations are largely explained by the AO index, with a r^2 of 44% during the period 1899–2001, suggesting that the Siberian High plays a very important role in Bohai Sea temperatures and sea ice conditions in the context of the planetary scale AO.

The AO is capable of impacting the Siberian SLP in both dynamical and thermal ways. The build up of the SLP high is mainly due to strong surface radiation cooling and partially due to the downward motion of air because of the middle troposphere convergence (Ding and Krishnamurti, 1987; Ding, 1990). Thompson and Wallace (2000) examined the role of heat advection in maintaining the surface air temperature anomalies associated with the AO. In high-AO winters, an anomalous warm temperature advection is found over much of the mid-high-latitudes of the Eurasian continent. The temperature advection balances the radiation cooling to some extent, leading to a lower SLP and a weaker Siberian High.

A weakening trend in SLP over Northern Hemispheric high latitudes in recent decades is dominant (Walsh *et al.*,

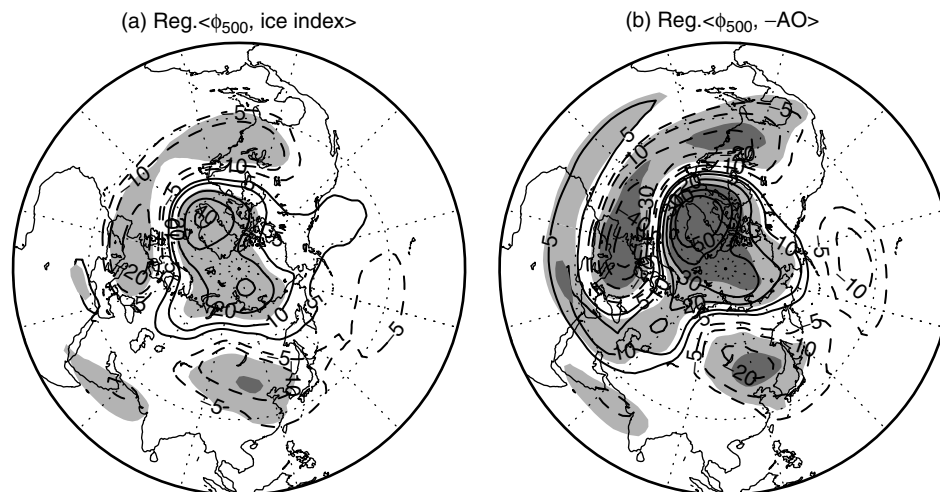


Figure 12. Changes of December–February 500 hPa heights in association with a one-standard-deviation stronger sea ice severity index (a) and a one-standard-deviation weaker AO (b), based on the data period of winters 1957/58–2001/02. Areas significant at the 0.05 level are shaded. High correlation center with $|r| \geq 0.6$ is indicated by darker shading. Contour intervals: ± 5 , ± 10 , ± 20 , ± 30 , ± 40 m. Zero contours are omitted for simplicity.

1996; Serreze *et al.*, 2000). For example, using different data sets and definitions, (Gong and Ho, 2002) and (Panagiotopoulos *et al.*, 2005) found that the Siberian High experienced a significant decrease of -1.78 hPa over 10 years from 1978–2000 and -2.5 hPa over 10 years between 1978 and 2001, respectively. These results are consistent with the rapid drop in pressure over the Arctic Ocean and neighboring areas (Walsh *et al.*, 1996), and the upward trend in AO and NAO in the last couple of decades (Hurrell, 1995; Thompson *et al.*, 2000). This suggests that the significant mitigation trend of the Bohai Sea ice severity could be linked to the AO-related SLP trend.

500 hPa heights

In order to understand the middle troposphere circulation changes in association with the Bohai Sea ice severity, we computed the regression of 500 hPa heights against the ice index (Figure 12). Significant negative height anomalies are located around the Bohai Sea with the correlation center appearing in the north area. Interestingly, negative signals are found simultaneously in the middle latitudes (about 30 – 60° N) of the North Pacific, southern Europe, the North Atlantic, and North America, while positive anomalies occur in the Arctic Ocean. Field significance test also suggests the patterns are significant at the 0.05 level. This structure obviously resembles the negative AO pattern, implying an AO influence in generating the planetary scale 500 hPa height anomalies over the extratropical Northern Hemisphere.

In the climatology of the area, a trough is situated in East Asia at the 500 hPa level. In Figure 12, negative height anomalies in East Asia imply that in low-AO winters the trough gets deeper and the meridional pressure/height gradient between the middle latitudes and the polar regions weakens in the East Asian sector. To quantitatively represent the geopotential gradient

and trough intensity, we defined a trough index as the geopotential height difference between two regions determined according to high correlation centers, as shown in Figure 12. The region in the south is 100 – 120° E, 40 – 45° N, while the polar region is set to 90 – 150° E, 70 – 85° N. To get rid of the influence of different variances between the middle and high latitudes, the polar and southern regions are normalized separately and then their difference (south minus north) is used as the trough index. There is a moderate correlation between the trough index and the AO, $r = +0.58$ ($r^2 = 34\%$ for the data period 1957/58–2001/02 and significant at the 0.01 level). When the trough index becomes higher, the air temperature around the Bohai Sea increases significantly, and the number of freezing days, FDDs and the length of freezing duration all show significant relations correspondingly (Table III).

There are several ways for the trough index to be linked to the AO-Bohai Sea temperature and ice conditions. In positive-AO phases the trough index rises, implying a shallower East Asian trough and greater gradient at the 500 hPa height from middle latitude Asia across the North Pole. This suggests that in association with the high-AO phases the meridional wind components of the air-flow are suppressed, providing unfavorable conditions for a cold air mass in polar and sub-polar regions bursting southward into East Asia. On the other hand, in low-AO winters an anomalous north wind occurs in most of the mid-high-latitudes of Asia in the middle to lower troposphere (such as 850 hPa level, see Figure 8).

In addition, a high-AO and high trough index means a shrinking circumpolar vortex over the East Asian sector, also providing unfavorable conditions for the activity of cold air mass. The Northern Hemisphere circumpolar vortex index can be defined as the area encompassed by a specific contour line, which is determined by the strongest meridional height gradient at the 500 hPa level (Burnett, 1993). The Asian polar vortex (with the

same earlier definition but over the sector 60–150°E, as employed by the China Meteorological Administration in routine weather analysis) is significantly correlated with mean temperature, $r = -0.54$ ($r^2 = 29\%$), NFD, $r = +0.53$ ($r^2 = 28\%$), FDD, $r = -0.52$ ($r^2 = 27\%$), and the length of freezing duration, $r = +0.48$ ($r^2 = 23\%$).

Dynamically, the varying trough can cause a simultaneous change in divergence in the relevant regions. The 500 hPa level divergence in association with the negative phase AO shows negative anomalies over most of middle-high Asia (figure not shown), implying an anomalous air-flow convergence in the rear of the East Asian trough, which helps in strengthening the surface pressure and consequently leads to a stronger Siberian High.

In short, these features of the middle troposphere (as represented by the 500 hPa level) are consistent with different circulation changes at other levels, and also display good correlation to the Bohai Sea temperatures and ice conditions with regard to the AO.

LONG-TERM CHANGES

It is interesting to analyze the long-term changes of the Bohai Sea ice severity during the last one hundred years in association with the AO under a rapidly warming global climate. Unfortunately, there is insufficient objective observation of the Bohai Sea ice conditions before the 1950s. Given the fact that ice conditions are tightly connected to the regional air temperature and large-scale atmospheric circulation systems, in this study we have provided an analysis of the meteorological coldness derived from the temperature and circulation indices since 1880.

First we reconstructed a historical Bohai Sea ice index using (1) regional mean temperatures, (2) the Siberian High index, and (3) a trough index. Winter mean temperature anomalies for Chaoyang, Tianjin, Dalian, and Yantai are available from 1880 (Table I). Their arithmetic averaging creates a regional mean temperature time series. The Siberian High index was computed using the HadSLP2 data available since 1850. The trough index was extended to 1880 using the Northern Hemisphere 500 hPa height reconstructions of Gong *et al.* (2006), which were reconstructed by using historical surface pressure and temperature data of the Climatic Research Unit of the University of East Anglia through a stepwise regression approach.

On the basis of the data for the period 1953/54–2001/02, the regional mean temperature time series, the Siberian High, and trough indices were used as independent variables and fitted to the observed Bohai Sea ice severity time series using a multivariate regression method. As the regression equation coefficients were determined, they were employed to compute the sea ice severity index for the period 1880–1952. These variables are of high consistency and their mutual relationships are stable with time (Table VII). In the earlier 54 years and the later 49 years, their mutual correlations are all significant and similar in the two periods. Therefore, the

Table VII. Correlation among historical time series of AO, Siberian High, trough index, and temperature for the period 1899–1952. Their relations for period 1953/54–2001/02 are shown in parentheses.

	AO	Siberian High	Trough index	Temperature
AO	+1.0	−0.72	+0.53	+0.70
Siberian High	(−0.60)	+1.0	−0.68	−0.86
Trough index	(+0.42)	(−0.71)	+1.0	+0.59
Temperature	(+0.58)	(−0.88)	(+0.64)	+1.0

All significant at $\alpha = 0.01$ level.

derived ice index statistics and their coherent association with the independent variables are very likely stationary over time. Using more predictors usually helps to increase the variance explained by the regression model. Here we intended to exclude the AO in the ice reconstruction for the purpose of analyzing the historical AO-sea-ice relationship (i.e. keep the sea ice reconstruction independent of AO). In fact, when the AO is included in the regression model, the total explained variance of ice severity varies slightly from 66.3% to 69.1%, an increase of only 2.8%, this is simply because AO has very high covariance with temperature, Siberian High, and trough index. Figure 13 shows the long-term time series of the ice severity along with other variables. It should be pointed out that the reconstruction of the ice severity index should be regarded as a meteorological cold severity index instead of the actual sea ice severity, although the correlation between the estimated sea ice index and the observation is as high as +0.84 ($r^2 = 71\%$) during the period 1953–2001.

In Figure 13, some high and low values of ice severity stand out. During 1880–1952, three winters of extremely heavy ice severity can be identified, namely, the winters of 1935/36, 1944/45, and 1946/47. All ice severity index anomalies are greater than 1.98σ . In the same period, two extremely low ice severity anomalies, with anomalies below -1.98σ , are identified, including 1934/35 and 1948/49. It is interesting to note that very heavy ice conditions were documented in local fishery logs in the winters of 1935/36 and 1946/47, which are the two years when almost the entire Bohai Sea was covered by sea ice (Bai *et al.*, 2001). Ice severities for these two winters are comparable to the winter of 1968/69. These winters are consistent with our reconstructed sea ice severity extremes.

In order to check the corresponding changes in SLP and 500 hPa heights in association with the historical ice severity extremes, we made some composite maps. To suppress the random noises, we analyzed the five highest and five lowest ice severity winters, instead of the three heavy and two light ice condition extremes as identified above. Figure 14 shows the difference of the heavy ice condition winters minus the light ice condition winters. The heaviest five years are 1935/36, 1944/45, 1946/47, 1896/97, and 1892/93, and the lightest five

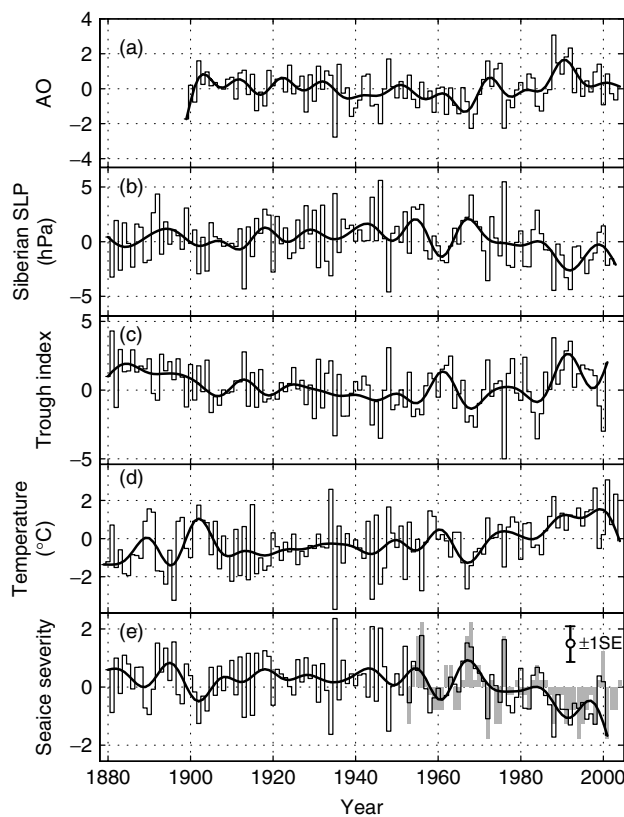


Figure 13. Long-term series of AO (a), Siberian High (b), trough index (c), and mean temperature (d) from four stations, and the computed sea ice severity (e). In (e), the observed sea ice severity values are superimposed as bars. Width of ± 1 standard error (SE) of the reconstructed ice severity index is shown together in the upper right corner. All presented as departures from the reference period of 1961–1990. Low-frequency variations are shown as smooth lines.

years include 1934/35, 1948/49, 1902/03, 1913/14, and 1915/16. Generally, the features in SLP and 500 hPa heights are very similar to the AO-related changes, as revealed by the regression relations of modern observations (cf Figures 11 and 12), although the composites are based on the historical SLP and reconstructed 500 hPa

heights. This supports the view that the AO also plays a notable role in these extreme ice conditions in the historical period.

During the last one hundred years, the AO-ice severity relationship has been stable through time, as revealed by the sliding correlations using a 30-year window. In almost all sub-time periods their correlations are significant, with one exception occurring around 1960 when the correlations were relatively low and slightly below the 0.05 level. The low correlations of AO around 1960 can also be found when it is compared with other variables (the Siberian High, the trough index, and regional temperature; Figure 13).

The possible links of the interannual and decadal timescale frequencies in the ice severity (Section 'Variation in sea ice severity') to the AO variability are checked using a cross-power spectral analysis. Cross-power coherence shows that the highest and significant covariances stand at about 2.1, 3, 7.5–14 year periods in the early period as well as during the entire data period. During the observation period since 1953, the variations of 2–2.5 years and ~ 8 years, are significant, and particularly, the secular trends in both series are dominant. Thus, the interannual and longer decadal signals of the AO in the Bohai Sea ice conditions are generally robust throughout the data period since the early 20th century.

It should be indicated that no evident trend is found in the ice index prior to the 1950s. The significant decline of ice severity after the 1970s is clearly unprecedented since at least 1880s. This trend is well in agreement with the enhancement of AO as well as the strong trends of the Siberian High SLP (-0.5 hPa over 10 years for the period 1970/71–2001/02), trough index ($+0.39$ over 10 years), and regional temperature ($+0.58$ °C over 10 years).

CONCLUSION

Located in the middle latitudes, the ice conditions of the Bohai Sea are very sensitive to the hemispheric climate

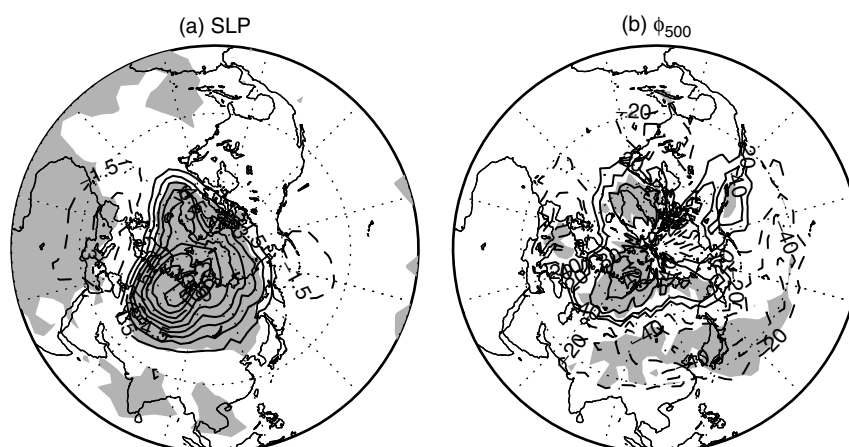


Figure 14. Composites of SLP and 500 hPa heights. Five heavy ice severity winters (1935/36, 1944/45, 1946/47, 1896/97, 1892/93) minus five light winters (1934/35, 1948/49, 1902/03, 1913/14, 1915/16). Contour interval for SLP is 1.5 hPa. Contour intervals for the 500 hPa level: ± 20 , ± 40 , ± 80 , ± 120 m. Zero contours are omitted for simplicity. Shading denotes significance at 0.05 level.

variability. In association with different phases of the AO, the regional mean temperature, number of freezing days, FDDs, and the length of freezing duration all change consistently, resulting in corresponding changes in the ice severity. In high-AO phases the Bohai Sea ice severity tends to be lighter, while in low-AO winters it is heavier.

Regional air temperature around the Bohai Sea shows significant differences in the mean as well as in the variance between high-AO and low-AO winters. There is a greater mean and smaller variance in high-AO winters than in low-AO years. In the context of ice severity, the change in the means is of greater importance than the variance. The changes in air temperature with regard to ice conditions are of a hemispheric scale and resemble the AO-related pattern of climate anomalies.

Large-scale circulation anomalies associated with the AO play an essential role in local temperatures and ice conditions. In high-AO phases, the SLP over mid-high-latitudes of the Eurasian continent tends to decrease and the East Asian trough gets shallower, mainly resulting from the anomalous surface heat advection, evidently causing weaker convergence in the middle troposphere, and weaker meridional wind anomalies in the lower troposphere. As a consequence, the Siberian High becomes weaker, and the East Asian air temperature rises above normal. Therefore the Bohai Sea ice severity diminishes. In contrast, heavier ice conditions tend to occur in low-AO winters.

Generally, the relationship between the AO and ice severity indices has been robust during the last one hundred years. Their covariance stand at about 2.1, 3, and 7.5–14 year periods. During the period 1880–1952, three winters of extremely heavy ice severity can be identified (namely, 1935/36, 1944/45, and 1946/47). The rapid decline in the Bohai Sea ice severity since the 1970s is unprecedented during the last century. This is well in agreement with the upward trend in the AO and the related changes of the Siberian High, trough index, and the regional air temperature.

The results presented in this study provide useful information about how the climate and sea ice of the middle latitudes respond to global climate changes in the context of the AO. The findings are also helpful for sea ice prediction, modeling, and assessments, and industrial management of the Bohai Sea region. However, the AO-temperature relation declines in the recent two decades, although their correlation is statistically significant. Whether and how this is associated with global warming needs further study.

ACKNOWLEDGEMENTS

This study was supported by the project 'Integrated research on the composition of polar atmosphere and climate change (COMPAC)' of the Korea Polar Research Institute (PE07030), NSFC-40675035, and the 111 Project. The ECMWF reanalysis data used in this study were obtained from the ECMWF server at <http://data.ecmwf.int>.

REFERENCES

- Allan RJ, Ansell TJ. 2006. A new globally complete monthly historical mean sea level pressure data set (HadSLP2): 1850–2004. *Journal of Climate* **19**(22): 5816–5842.
- Ambaum MHP, Hoskins BJ, Stephenson DB. 2001. Arctic oscillation or North Atlantic oscillation? *Journal of Climate* **14**: 3495–3507.
- Bai S, Liu Q-Z, Li H, Wu H-D. 1999. Sea ice in the Bohai Sea of China. *Marine Forecasts* **16**(3): 1–9, (in Chinese).
- Bai S, Liu Q-Z, Wu H-D, Wang Y-L. 2001. Relation of ice conditions to climate change in the Bohai Sea of China. *Acta Oceanologica Sinica* **20**(3): 331–342.
- Brauch JP, Gerdes R. 2005. Response of the northern North Atlantic and Arctic oceans to a sudden change of the North Atlantic oscillation. *Journal of Geophysical Research* **110**(C11018): Doi:10.1029/2004JC002436.
- Bretherton C, Widmann M, Dymnikov VP, Wallace JM, Bladé I. 1999. The effective number of spatial degrees of freedom of a time-varying field. *Journal of Climate* **12**: 1990–2009.
- Burnett AW. 1993. Size variations and long-wave circulation within the January northern hemisphere circumpolar vortex: 1946–89. *Journal of Climate* **6**: 1914–1920.
- Chen W, Takahashi M, Graf H-F. 2003. Interannual variations of stationary planetary wave activity in the northern winter troposphere and stratosphere and their relations to NAM and SST. *Journal of Geophysical Research* **108**(D24): 4797, Doi:10.1029/2003JD003834.
- Deser C, Walsh JE, Timlin MS. 2000. Arctic sea ice variability in the context of recent atmospheric circulation trends. *Journal of Climate* **13**: 617–633.
- Dickson RR, Osborn TJ, Hurrell JW, Meincke J, Blindheim J, Adlandsvik B, Vinje T, Alekseev G, Maslowski W. 2000. The Arctic ocean response to the North Atlantic oscillation. *Journal of Climate* **13**(15): 2671–2696.
- Ding Y-H. 1990. Buildup, air-mass transformation and propagation of Siberian High and its relations to cold surge in East Asia. *Meteorology and Atmospheric Physics* **44**: 281–292.
- Ding Y-H, Krishnamurti TN. 1987. Heat budget of the Siberian high and the winter monsoon. *Monthly Weather Review* **115**: 2428–2449.
- Geng S-Q, Wang X. 2001. Sea ice in the Bohai sea during La Niña years. *Marine Science Bulletin* **20**(2): 1–11, (in Chinese).
- Gong D-Y, Wang S-W. 1999a. 1998: The warmest year on record in China. *Meteorologic Monthly* **25**(8): 1–3.
- Gong D-Y, Wang S-W. 1999b. Long-term variability of the Siberian high and the possible influence of global warming. *Acta Geographica Sinica* **54**(2): 125–133, (in Chinese).
- Gong D-Y, Ho C-H. 2002. Siberian High and climate change over middle to high latitude Asia. *Theoretical and Applied Climatology* **72**: 1–9.
- Gong D-Y, Ho C-H. 2004. Intra-seasonal variability of wintertime temperature over East Asia. *International Journal of Climatology* **24**(2): 131–144.
- Gong D-Y, Wang S-W, Zhu J-H. 2001. East Asian winter monsoon and Arctic oscillation. *Geophysical Research Letters* **28**: 2073–2076.
- Gong D-Y, Wang S-W, Zhu J-H. 2004. Arctic oscillation influence on daily temperature variance in winter over China. *Chinese Science Bulletin* **49**(6): 637–642.
- Gong D-Y, Drange H, Gao Y-Q. 2006. Reconstruction of northern hemisphere 500 hPa geopotential heights back to the late 19th century. *Theoretical and Applied Climatology* Doi:10.1007/s00704-006-0271-3, (In press - online first).
- Gu W, Shi P-J, Liu Y, Xie F, Cai X-P. 2002. The characteristics of temporal and spatial distribution of negative accumulated temperature in Bohai Sea and north Yellow Sea. *Journal of Natural Resources* **17**(2): 168–173, (In Chinese).
- Gu W, Zhang Q-Y, Xie F, Li N, Cui W-J. 2003. Estimation of the amount of sea ice resources in Liaodong gulf by climate statistics. *Resources Science* **25**(3): 9–16, (in Chinese).
- Houghton JT, Ding Y-H, Griggs DJ, Noguer M, van der Linden PJ, Dai X-S, Maskell K, Johnson CA. 2001. *Climate Change 2001: The Scientific Basis. Contribution of Working Group I to the Third Assessment Report of the Intergovernmental Panel on Climate Change*. Cambridge University Press: Cambridge, 881.
- Hurrell JW. 1995. Decadal trends in the North Atlantic oscillation: regional temperatures and precipitation. *Science* **269**: 676–679.
- Hurrell JW. 1996. Influence of variations in extratropical wintertime teleconnections on northern hemisphere. *Geophysical Research Letters* **23**: 665–668.

- Hurrell JW, van Loon H. 1997. Decadal variations in climate associated with the North Atlantic oscillation. *Climatic Change* **36**(3–4): 301–326.
- Jeong JH, Ho CH. 2005. Changes in occurrence of cold surges over East Asia in association with Arctic oscillation. *Geophysical Research Letters* **32**(L14704): Doi:10.1029/2005GL023024.
- Jevrejeva S, Moore JC. 2001. Singular spectrum analysis of Baltic Sea ice conditions and large-scale atmospheric patterns since 1708. *Geophysical Research Letters* **28**(4503C): 4507.
- Jevrejeva S, Moore JC, Grinsted A. 2003. Influence of the Arctic oscillation and El Niño-Southern Oscillation (ENSO) on ice conditions in the Baltic Sea: the wavelet approach. *Journal of Geophysical Research* **108**(D21): 4677, Doi:10.1029/2003JD003417.
- Johannessen OM, Bengtsson L, Miles M, Kuzmina SI, Semenov V, Alekseev GV, Nagurny AP, Zakharov VF, Bobylev LP, Pettersson LH, Hasselmann K, Cattle HP. 2004. Arctic climate change: observed and modelled temperature and sea-ice variability. *Tellus* **56A**(4): 328–341.
- Koslowski G, Glaser R. 1999. Variations in reconstructed ice winter severity in the western Baltic from 1501 to 1995, and their implications for the North Atlantic oscillation. *Climatic Change* **41**: 175–191.
- Kwok R, Rothrock DA. 1999. Variability of Fram Strait ice flux and North Atlantic oscillation. *Journal of Geophysical Research* **104**(C3): 5177C5190.
- Li Z-J. 1999. An field investigation of sea ice in Liaodong bay. *Marine Forecasts* **16**(3): 48–55, (in Chinese).
- Li J, Huang J-Y, Liu Q-Z. 2005. The long-term variation characteristics of sea ice in the Bohai Sea and the north Huanghuai Sea. *Marine Forecasts* **22**(2): 22–32, (in Chinese).
- Lindsay RW, Zhang J. 2005. The thinning of Arctic sea ice, 1988–2003: have we passed a tipping point? *Journal of Climate* **15**: 4879–4894.
- Liu Q-Z, Huang J-Y, Bai S, Wu H-D. 2004. Studies on the causation of sea ice decadal variation in the Bohai Sea of China. *Acta Oceanologica Sinica* **26**(2): 11–19, (in Chinese).
- Meier W, Stroeve J, Fetterer F, Knowles K. 2005. Reductions in Arctic sea ice cover no longer limited to summer. *EOS* **86**(36): 326–327.
- Meng S, Li H. 1999. Weather, climate, and sea ice in Bohai sea in 1998/99. *Marine Forecasts* **16**(4): 52–59, (in Chinese).
- Overland JE. 2005. The arctic climate paradox: the recent decrease of the Arctic oscillation. *Geophysical Research Letters* **32**(6): L06701.
- Panagiotopoulos F, Shahgedanova M, Hannachi A, Stephenson DB. 2005. Observed trends and teleconnections of the Siberian high: a recently declining center of action. *Journal of Climate* **18**(9): 1411C1422.
- Parkinson CL, Cavalieri DJ, Gloersen P, Zwally HJ, Comiso JC. 1999. Arctic Sea ice extents, areas, and trends, 1978–1996. *Journal of Geophysical Research* **104**: 20837–20856.
- Polyakov I, Alekseev G, Bekryaev R, Bhatt U, Colony R, Johnson M, Karklin V, Makshtas A, Walsh D, Yulin A. 2002. Observationally based assessment of polar amplification of global warming. *Geophysical Research Letters* **29**(18): 1878–1881.
- Rigor IG, Wallace JM, Colony RL. 2002. Response of sea ice to the Arctic oscillation. *Journal of Climate* **15**(18): 2648–2663.
- Rothrock DA, Zhang J. 2005. Arctic ocean sea ice volume: what explains its recent depletion? *Journal of Geophysical Research* **110**: C01002, Doi:10.1029/2004JC002282.
- Serreze MC, Francis JA. 2006. The Arctic amplification debate. *Climatic Change* **76**(3–4): 241–264.
- Serreze MC, Walsh JE, Chapin FS III, Osterkamp T, Dyurgerov M, Romanovsky V, Oechel WC, Morison J, Zhang T, Barry RG. 2000. Observation evidence of recent change in the northern high-latitude environment. *Climatic Change* **46**: 159–207.
- Shi P-J. 2003. *Atlas of Natural Disaster System of China*. Science Press: Beijing, 218.
- SOA. 1974. Sea ice in Bohai and northern Yellow Seas (I). (The State Oceanic Administration of Peoples Republic of China, Data Collection).
- Stroeve JC. 2005. Tracking the Arctic's shrinking ice cover: another extreme September minimum in 2004. *Geophysical Research Letters* **32**(4): L04501.
- Thompson DWJ, Wallace JM. 1998. The Arctic oscillation signature in the wintertime geopotential height and temperature fields. *Geophysical Research Letters* **25**: 1297–1300.
- Thompson DWJ, Wallace JM. 2000. Annular modes in the extratropical circulation, part I: Month-to-month variability. *Journal of Climate* **13**(5): 1000–1016.
- Thompson DWJ, Wallace JM, Hegerl GC. 2000. Annular modes in the extratropical circulation, part II: Trends. *Journal of Climate* **13**(5): 1018–1036.
- Uppala SM, Kallberg PW, Simmons AJ, Andrae U, da Costa Bechtold V, Fiorino M, Gibson JK, Haseler J, Hernandez A, Kelly GA, Li X, Onogi K, Saarinen S, Sokka N, Allan RP, Andersson E, Arpe K, Balmaseda MA, Beljaars ACM, van de Berg L, Bidlot J, Bormann N, Caires S, Chevallier F, Dethof A, Dragosavac M, Fisher M, Fuentes M, Hagemann S, Holm E, Hoskins BJ, Isaksen I, Janssen PAEM, Jenne R, McNally AP, Mahfouf J-F, Morcrette J-J, Rayner NA, Saunders RW, Simon P, Sterl A, Trenberth KE, Untch A, Vasiljevic D, Viterbo P, Woollen J. 2005. The ERA-40 re-analysis. *Quarterly Journal of the Royal Meteorological Society* **131**: 2961–3012.
- Walsh JE, Chapman WL, Shy TL. 1996. Recent decrease of sea level pressure in the central Arctic. *Journal of Climate* **9**: 480–486.
- Wang S-W, Gong D-Y. 2000. Enhancement of the warming trend in China. *Geophysical Research Letters* **27**(16): 2581–2584.
- Wang S-W, Gong D-Y, Zhu J-H. 2001. Twentieth-century climatic warming in China in the context of the Holocene. *The Holocene* **11**(3): 313–321.
- Wu B-Y, Wang J. 2002. Winter Arctic oscillation, Siberian high and East Asian winter monsoon. *Geophysical Research Letters* **29**: 1897, Doi:10.1029/2002GL015373.
- Wu B, Wang J, Walsh JE. 2006. Dipole anomaly in the winter Arctic atmosphere and its association with sea ice motion. *Journal of Climate* **19**(2): 210–225.
- Yang G-J. 2000. Bohai Sea ice conditions. *Journal of Cold Regions Engineering* **14**(2): 54–67.
- Zhang F-J. 1986. *Sea ice in China*. China Ocean Press: Beijing.
- Zhang Q-W, Li B-H. 1999. Bohai Sea ice condition in 1998/99 and comparison with other winters. *Marine Forecasts* **16**(2): 79–86, (in Chinese).